How to cite: *Angew. Chem. Int. Ed.* **2021**, *60*, 3277–3282
International Edition: doi.org/10.1002/anie.202013713
German Edition: doi.org/10.1002/ange.202013713

Electrocatalysis

Flow Electrolyzer Mass Spectrometry with a Gas-Diffusion Electrode Design

Bjorn Hasa, Matthew Jouny, Byung Hee Ko, Bingjun Xu, and Feng Jiao**

Abstract: *Operando mass spectrometry is a powerful technique to probe reaction intermediates near the surface of catalyst in electrochemical systems. For electrochemical reactions involving gas reactants, conventional operando mass spectrometry struggles in detecting reaction intermediates because the batch-type electrochemical reactor can only handle a very limited current density due to the low solubility of gas reactant(s). Herein, we developed a new technique, namely flow electrolyzer mass spectrometry (FEMS), by incorporating a gas-diffusion electrode design, which enables the detection of reactive volatile or gaseous species at high operating current densities (> 100 mA cm^{-2}). We investigated the electrochemical carbon monoxide reduction reaction (eCORR) on polycrystalline copper and elucidated the oxygen incorporation mechanism in the acetaldehyde formation. Combining FEMS and isotopic labelling, we showed that the oxygen in the as-formed acetaldehyde intermediate originates from the reactant CO, while ethanol and n-propanol contained mainly solvent oxygen. The observation provides direct experimental evidence of an isotopic scrambling mechanism.*

Introduction

Since Hori's pioneering work more than three decades ago,[1] electrochemical CO_2 reduction reaction (eCO_2RR) in aqueous solution has received considerable attention for the production of chemicals and fuels.[2] Among all electrocatalysts, copper (Cu) is the only metal capable of producing significant amounts of multicarbon (C_{2+}) products, such as hydrocarbons and oxygenates,[3–6] though further enhancement in its selectivity for valuable products is required for practical applications.[7] A molecular level understanding of the reaction mechanism on Cu could enable the rational design of more selective catalysts toward the desired C_{2+} products. While coupling of adsorbed CO has been proposed as the rate determining step in the formation of multicarbon products in eCO_2RR, reaction pathways leading to the observed C_{2+} oxygenates and hydrocarbons, as well as handles for selectivity control, remain a topic of considerable discussion. Acetaldehyde is considered as a key intermediate to ethanol via a facile electrochemical reduction step.[8,9] It is also proposed as a potential intermediate in the formation of n-propanol via coupling with CO, followed by electrochemical reduction. However, our recent work showed while C–C coupling between acetaldehyde and CO did occur on Cu, it was unlikely to be the main pathway to n-propanol.[10] Recent studies showed that solvent oxygen was incorporated into ethanol and n-propanol. Two potential explanations have been put forward: O exchange between acetaldehyde and water, and a solvent-based concerted hydrolysis mechanism where both oxygen atoms from CO are removed from the adsorbed intermediate.[11–13] Direct evidence supporting either interpretation has been lacking. The difficulty in conclusively elucidating the potential roles acetaldehyde plays in eCO_2RR on Cu could be attributed at least in part to its reactive nature even though its production starts at low overpotentials.[14,15] Previous studies suggest that the detection of acetaldehyde is difficult by proton nuclear magnetic resonance (NMR) due to the multiple efficient pathways through which acetaldehyde could be further converted, e.g., Cannizzaro reaction, Aldol condensation and Tishchenko reaction, especially in highly alkaline electrolytes.[5,14] Thus, online detection of reactive intermediates such as acetaldehyde during reaction could be especially informative in mechanistic investigations.

Combined with an electrochemical cell, mass spectrometry (MS) is a promising technique to probe reactive species at the electrode-electrolyte interface. To date, several *operando*/in situ electrochemical MS techniques, such as differential electrochemical mass spectrometry (DEMS),[9] on-line electrochemical mass spectrometry (OLEMS),[16] electrochemical real-time mass spectrometry (EC-RTMS),[17] and selected-ion flow tube mass spectrometry (SIFT-MS),[18] have been developed to elucidate mechanistic pathways for eCO_2RR. Regardless of the detailed design of each technique, CO_2 is invariably introduced to the electrochemical cell using a CO_2-saturated liquid electrolyte, which greatly limits the capability of the techniques. For example, due to the low solubility of CO_2 in aqueous electrolytes (approximately 30 mM), the highest eCO_2RR current density that can be achieved using a CO_2-saturated aqueous electrolyte is approximately 40 mA cm^{-2}, which is far below industrially relevant current densities (> 100 mA cm^{-2}). This gap in the operating current density is important for mechanistic studies for two reasons: 1) a higher current density leads to a higher concentration of intermediates, which could enable the detection of reactive species; and 2) the dominant reaction pathway could be current density dependent. Further, the

[*] B. Hasa, M. Jouny, B. H. Ko, B. Xu, F. Jiao
Center for Catalytic Science and Technology, Department of Chemical and Biomolecular Engineering, University of Delaware
Newark, DE 19716 (USA)
and
E-mail: jiao@udel.edu
bxu@udel.edu

Supporting information (all data needed to evaluate the conclusions in the paper are present in the paper and/or the Supporting Information) and the ORCID identification number(s) for the author(s) of this article can be found under: https://doi.org/10.1002/anie.202013713.

maximum operating current density would be much lower for gases with a lower solubility than CO_2, e.g., CO and N_2, making it difficult to obtain useful information using the existing electrochemical MS techniques.

In this work, we design and construct a one-of-its-kind membrane-less flow electrolyzer mass spectrometry (FEMS), which features a gas-diffusion electrode (GDE) design to overcome the mass transport limitations of gas reactant delivery to the catalyst surface. This design allows direct introduction of gaseous reactants, e.g., CO_2 and CO, to the electrode surface without equilibrating with the electrolyte, thus circumventing the technical challenges of existing electrochemical MS techniques. To demonstrate the capability of FEMS in mechanistic investigations, we employ the electrochemical CO reduction reaction (eCORR) as a model reaction. A series of eCORR experiments on polycrystalline Cu with isotopically labelled compounds at a current density of 150 mA cm^{-2} show that the oxygen in acetaldehyde produced electrochemically originates from CO. Acetaldehyde goes through a rapid oxygen exchange with H_2O in the electrolyte, followed by an electroreduction reaction to form ethanol, leading to the incorporation of the oxygen atom from H_2O in the produced alcohol. Further, coupling between acetaldehyde and CO to n-propanol at the current density of 150 mA cm^{-2} is shown to be less populated pathway than a previous study using a batch cell at much lower current densities.

Results and Discussion

FEMS analysis and mass deconvolution procedure. A schematic diagram of the GDE-based FEMS design is shown in Figure 1. The cathode GDE is prepared by spray coating commercial Cu nanoparticles (average diameter ≈25 nm) on a carbon gas diffusion layer (GDL) with a typical Cu loading of 0.3 mg cm^{-2} (experimental setup and physicochemical characterization of the prepared electrodes are provided in the Supporting Information (S.I), Figures S2,3). The CO gas is fed to the hydrophobic side of the GDL, whereas the Cu catalyst layer faces a liquid electrolyte chamber. For the anode GDE, IrO_2 particles are coated onto a GDL, which is slightly smaller than that on the cathode side to provide space for the capillary probe of the MS. The tip of the probe is covered by a porous polytetrafluoroethylene (PTFE) membrane with an average pore size of 200 μm and placed in close contact with the Cu catalyst layer (Figure 1) to probe the species generated from the catalyst layer during reaction. The capillary probe is located close to the gas inlet to minimize convolution of species generated locally and upstream. No ion exchange membrane is employed in the electrochemical cell. More details regarding the FEMS setup can be found in the Method section and S.I.-1.

The high current densities afforded by the GDE design enable the detection of reactive species in the eCORR. At a constant CO feeding rate of 5 mL min^{-1}, the electrochemical cell is operated at 10, 20, 35, 100, and 150 mA cm^{-2}. In general, the overall MS signals positively correlate with the current density (Figure S18 shows the mass signals of all products during eCORR). Because the eCORR products share many common mass fragments, such as -CH_3^+ ($m/z = 15$), -CH_2OH^+ ($m/z = 31$), CH_3CO^+ ($m/z = 43$), and $CH_3CH_2O^+$ ($m/z = 45$), reliable deconvolution of MS signals into contributions from various species is critical to the product analysis. Mass fragmentation patterns of all species used in the deconvolution are obtained with neat samples. The detailed deconvolution procedure of the selected masses is shown in SI-2, which ensures that the sum of the contributions from mass

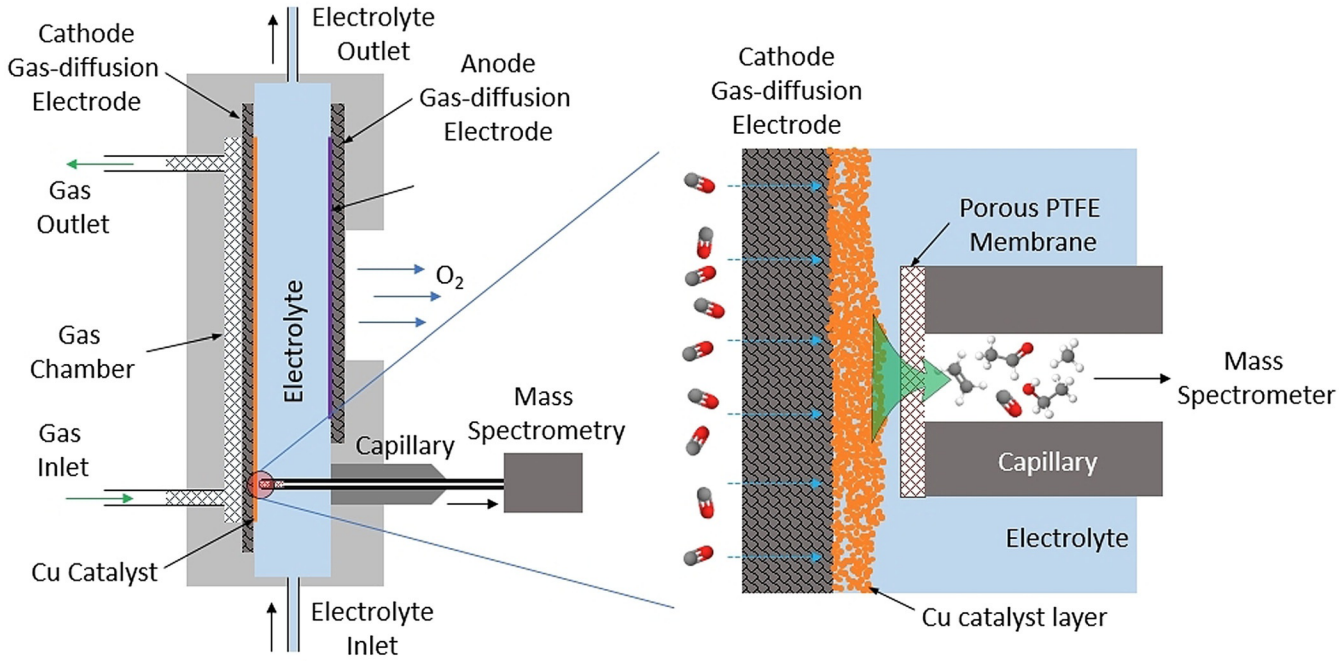

Figure 1. Schematic of the GDE design of flow electrolyzer mass spectrometry.

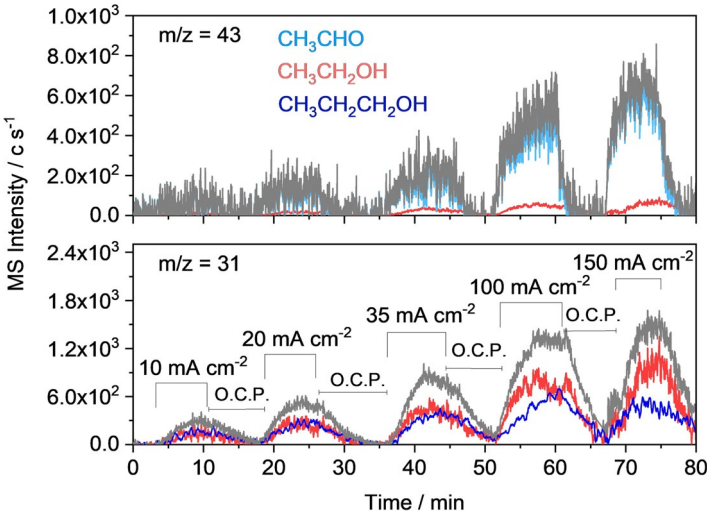

Figure 2. Deconvoluted MS signals for eCORR products. The grey lines represent the total MS signals at m/z 31 and 43. The signals of FEMS at various current densities are obtained in 1 M KOH electrolyte at a CO flow rate of 5 mL min^{-1}. Applied current densities are indicated in the lower panel and O.C.P. stands for the open circuit potential.

fragments with a specific mass-to-charge ratio (m/z) from all species is identical to the recorded MS signal. As an example, acetaldehyde, ethanol and n-propanol contribute 90%, 9% and ≈1%, respectively, to the $m/z = 43$ signal (Figure 2) at relatively high current densities (> 35 mA cm^{-2}), whereas the signal-to-noise ratios at lower current densities are too low to perform reliable deconvolution. The signal-to-noise ratio of $m/z = 31$ signals (Figure 2) is substantially better than that of $m/z = 43$ even at lower current densities. At less than 35 mA cm^{-2}, ethanol and n-propanol signals contribute roughly equally to the $m/z = 31$ signal. As the current density increases to 100 mA cm^{-2}, the ethanol contribution becomes slightly higher than that from n-propanol, suggesting that the relative selectivity of n-propanol over ethanol decreases as the current density increases over 35 mA cm^{-2}. The downward trend of n-propanol selectivity at higher overpotentials, and correspondingly higher current densities, in the eCORR has been observed experimentally in the literature,[11] confirming the reliability of the data analysis method employed in this work. We note that the current density of this work (up to 150 mA cm^{-2}) is approximately 25 times higher than what can be achieved in a CO-saturated aqueous electrolyte using state-of-the-art electrochemical MS techniques.[19]

The origin of oxygen in oxygenates. To demonstrate the capability of FEMS in mechanistic investigations, we investigated the incorporation of oxygen in the electrolyte into the oxygenated products in the eCORR. Recently, several research groups reported the incorporation of oxygen from water into the oxygenated products in the eCO_2RR and eCORR based on isotopic labelling experiments and computational modeling.[12,13] In the proposed reaction mechanism of the eCORR (Figure 3a), an important step is the oxygen exchange between acetaldehyde and water catalyzed by hydroxide in a highly alkaline environment. However, the rapid oxygen exchange process makes the detection of as-produced acetaldehyde difficult for ex-situ techniques such as ^{1}H NMR. We use FEMS to probe the isotopic composition of the produced acetaldehyde with $H_2{}^{18}O$ in the electrolyte at a current density of 150 mA cm^{-2} (Figure 3b and 3c). The grey dash traces indicate the transition between regular $H_2{}^{16}O$ and labeled $H_2{}^{18}O$. The increase of the MS signal corresponding to $m/z = 33$ (-$CH_2{}^{18}OH^+$) with the switching from $H_2{}^{16}O$ to $H_2{}^{18}O$ suggests the incorporation of ^{18}O from $H_2{}^{18}O$ into ethanol. The peak intensity of the $m/z = 33$ signal is approximately 50% lower than that of the $m/z = 31$ signal in regular water. In addition, after switching to $H_2{}^{18}O$, the $m/z = 31$ signal decreases by ≈35%. Control experiment (Figure S21) indicates that 53% of $H_2{}^{16}O$ in the flow cell is replaced by $H_2{}^{18}O$ 5 min after the switch. Therefore, the decent match among the percentage of $H_2{}^{18}O$ in the electrolyte, the increase in the $m/z = 33$ signal (-$CH_2{}^{18}OH^+$) and the decrease in the $m/z = 31$ signal upon switching to the $H_2{}^{18}O$-containing electrolyte suggests that the oxygen in the produced ethanol largely originates from the electrolyte. The decrease in the intensity of the $m/z = 43$ signal (mainly CH_3CO^+) is less substantial, by approximately 35% after switching from $H_2{}^{16}O$ to $H_2{}^{18}O$ (Figure 3c). Although m/z 31 and 43 signals show similar level of decrease after the switch, this should not be interpreted as evidence of oxygen exchange into acetaldehyde. This is because the m/z 43 signal has contributions from both CH_3CHO, CH_3CH_2OH and $CH_3CH_2CH_2OH$, the incorporation of ^{18}O in any of these compound would lead to a decline of the signal. Since the intensity ratio of m/z 31 and m/z 43 in CH_3CH_2OH and $CH_3CH_2CH_2OH$ are relatively similar (Figure S13), their combined contribution in m/z 43 can be estimated. The m/z 43 signal attributable to acetaldehyde only declines by 15% after the switch, which is smaller than that of the m/z 31 signal. The relatively poor signal to noise ratio of the m/z 43 signal makes a definitive claim difficult. The slight decrease of the signal 45 suggest that the oxygen in acetaldehyde originates from CO while that in ethanol is scrambled with water, which is consistent with the proposed oxygen exchange mechanism.[11] The observed oxygen exchange between as-produced acetaldehyde and H_2O in the eCORR is further examined using a stationary labeled $H_2{}^{18}O$ electrolyte, i.e., the electrolyte does not change/flow during the experiment. Consistent with results obtained from the $H_2{}^{16}O/H_2{}^{18}O$ switching experiment (Figures 3b,c), the majority of the as-produced acetaldehyde (65%) does not contain ^{18}O in the static electrolyte with $H_2{}^{18}O$, supporting the hypothesis that the oxygen in acetaldehyde initially formed on the Cu catalyst surface likely comes from CO rather than H_2O (see Figures S23, 24, SI-4 for more details). Importantly, the increase of the $m/z = 57$ signal and the unchanged $m/z = 59$ signal (Figure S23) indicate that allyl alcohol contains only oxygen from CO. These results show a strong relation between solvent water and ethanol and n-propanol but no correlation with allyl alcohol. Similar results are also reported in the literature.[12] However, the oxygen incorporation into acetaldehyde formation has not previously been described in similar experimental studies (Figure S24).

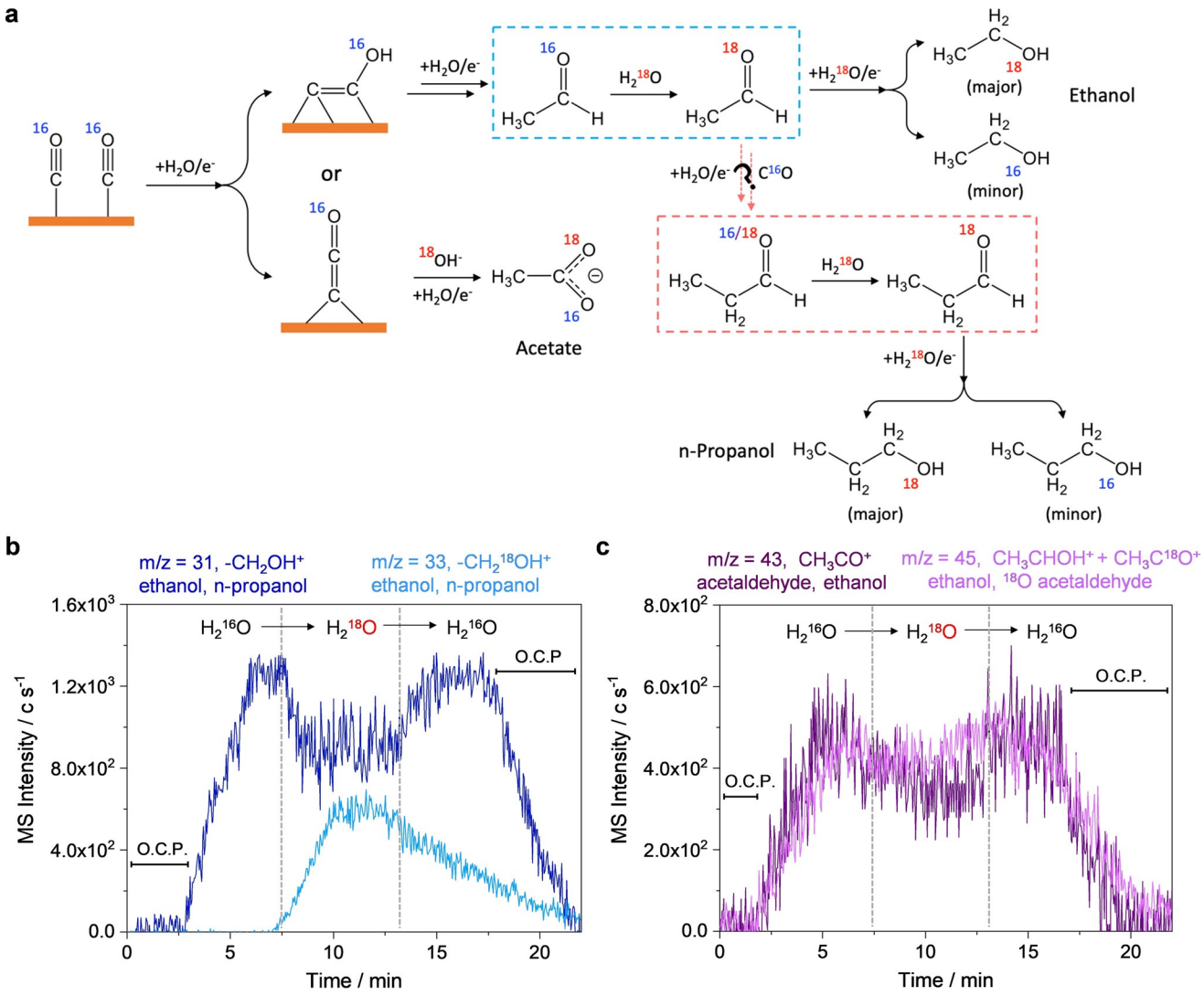

Figure 3. a) Proposed mechanism for the eCORR to oxygenated products. b),c) The FEMS fragments obtained in H_2O (0–7.5 and 12.5–22 minutes) and $H_2{}^{18}O$ (7.5–12.5 minutes). Unlabeled and labeled with ^{18}O fragments, $-CH_2OH^+$ (dark blue line) and $-CH_2{}^{18}OH^+$ (light blue line) (b). Mass to charge ratio 43 corresponding to the unlabeled fragment $-CH_3CO^+$ (purple line) and the m/z 45 corresponding to the labeled $-CH_3C^{18}O^+$ and unlabeled CH_3CHOH^+ fragments (c). CO reduction was conducted in 1 M KOH (flow rate 1 mL min^{-1}) at 150 mA cm^{-2} ($E \approx -1.15$ V (vs. RHE), see Figure S7b) and CO flow rate of 5 mL min^{-1}.

Further eCORR experiments using isotopic labeled $C^{18}O$ at a fixed current density of 150 mA cm^{-2} provide additional evidence supporting the proposed oxygen exchange mechanism. The electrochemical cell is first operated with $C^{16}O$, and then switched to $C^{18}O$ for approximately 8 minutes before switching back to the $C^{16}O$ feed. In Figure 4a, the $m/z = 33$ signal does not increase substantially upon switching to the $C^{18}O$ feed, suggesting that the ethanol produced from eCORR predominantly contains oxygen from H_2O rather than CO. This is in good agreement with the observation in the ^{18}O labeled water experiment (Figure 3b,c). The sharp increase in the $m/z = 31$ signal upon switching to the $C^{18}O$ feed is attributed to the natural isotope abundance of ^{13}C in $C^{18}O$ signal (1.8% according to control experiments, see Figure S25), which has a mass-to-charge ratio of 31 ($^{13}C^{18}O$). When switching to $C^{18}O$, an sharp decrease in the $m/z = 43$ signal is accompanied by the increase in the $m/z = 45$ signal (Figure 4b), which is likely associated with the fragments of $-CH_3C^{18}O$ (derived from $CH_3CH^{18}O$) and $CH_3CH^{16}OH^+$ (derived from $CH_3CH_2{}^{16}OH$ as a result of oxygen exchange with $H_2{}^{16}O$). Since O in ethanol comes primarily from the electrolyte, the $C^{16}O/C^{18}O$ switch is not expected to impact ethanol's contribution to the m/z 45 signal. Thus, the increase in the m/z 45 signal could be attributed to $CH_3CH^{18}O$. All the $C^{18}O$ labeled results are consistent with the observations in the $H_2{}^{18}O$ experiments and the proposed reaction mechanism in Figure 3. We note that although acetate is also a major C_2 product in the CORR, it cannot be detected by FEMS because it is not volatile.

Reaction mechanism of C_3 products. Turning to the C_3 products, i.e., propionaldehyde and n-propanol, in the eCORR, the formation mechanism on Cu catalysts has not been extensively studied in the literature (Figure 3a). A recent report showed that electroreductive coupling between

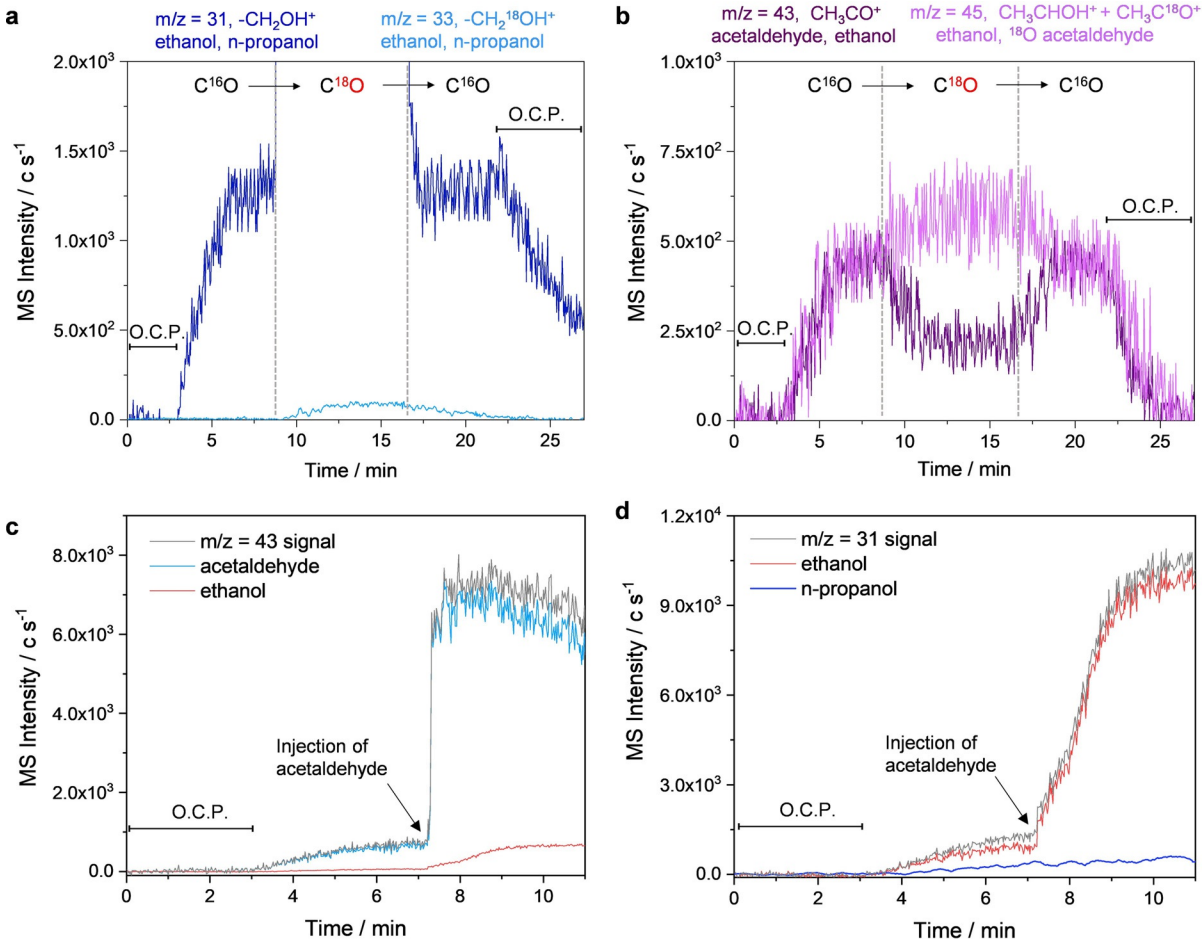

Figure 4. FEMS mass fragments during CO electrolysis. a),b) The mass fragments which correspond to the formation of ethanol and acetaldehyde during CO and $C^{18}O$ reduction. Unlabeled ($-CH_2OH^+$, dark blue line) and labeled ($-CH_2{}^{18}OH^+$, light blue line) ethanol signals (a). Unlabeled acetaldehyde ($-CH_3CO^+$, purple line) and labeled acetaldehyde ($-CH_3{}^{18}CO^+$) and unlabeled ethanol ($CH_3CH_2OH^+$) (pink line) (b). c),d) Effect of acetaldehyde reduction on the ethanol production rate. Deconvolution of the signals *m/z* 43 (c) and 31 (d). Electrolysis was conducted at KOH concentration 1 M, electrolyte flow rate 1 mL min^{-1}, constant current density of 150 mA cm^{-2} ($E \approx -1.1$ V (vs. RHE), see Figure S29), and reactant flow rate 5 mL min^{-1}. Acetaldehyde (200 mM) was added after 7 minutes.

CO and acetaldehyde did occur on Cu, however, it was unlikely to be the main pathway for the n-propanol formation in the eCORR.[10] Proionaldehyde was not detected due to the use of ex-situ proton NMR as the analytic method in that work. To investigate the reaction mechanism associated with the C_3 formation, we examine whether the reaction between acetaldehyde and CO promotes the production of propionaldehyde and n-propanol. MS signals of *m/z* both 43 and 31 are monitored at open circuit potential for 3 minutes, before applying a constant current density of 150 mA cm^{-2} under a constant flow of CO feed. A 200 mM of acetaldehyde is introduced after the MS signals stabilize (reaction time = 7 minutes in Figures 4c,d) through the liquid electrolyte solution. Upon introducing acetaldehyde, sharp increases are observed in the signals with *m/z* values of both 31 and 43 (Figures 4c,d). The jump in the *m/z* 43 signal is largely attributed to added acetaldehyde, with a minor contribution from the ethanol produced via the reduction of acetaldehyde (Figure 4c). Deconvoluted *m/z* = 31 signals show that the formation rate of n-propanol is not visibly impacted by the acetaldehyde addition, suggesting the coupling between acetaldehyde with CO is not a major pathway for n-propanol production.[10]

Conclusion

In summary, we showed that the incorporation of a gas diffusion electrode in the mass spectrometry enables a unique capability to probe reactive intermediates at high reaction rates (i.e., > 100 mA cm^{-2}) even for poorly soluble gas reactant, such as CO. Coupling with isotopic labeling experiments, we demonstrated the capability of FEMS to elucidate the reaction mechanism of Cu-catalyzed CO electroreduction. The results show clear evidence that the oxygen in the as-produced acetaldehyde is originated from CO feed, which is subsequently exchanged with the oxygen in the aqueous electrolyte (i.e., H_2O). Further studies show that ethanol is produced from the electroreduction of acetaldehyde, while the cross-coupling between CO and acetaldehyde does not promote the formation of C_3 products in any significant ways, suggesting that the C_2 intermediate that is involved in the

initial C_3 intermediate formation is not acetaldehyde but a species prior to the formation of acetaldehyde.

Acknowledgements

F.J. thanks the National Science Foundation for financial support (Award No. CBET-1904966).

Conflict of interest

The authors declare no conflict of interest.

Keywords: CO reduction · CO_2 utilization · electrocatalysis · operando mass spectrometry

[1] Y. Hori, K. Kikuchi, S. Suzuki, *Chem. Lett.* **1985**, *14*, 1695 – 1698.
[2] S. Nitopi, E. Bertheussen, S. B. Scott, X. Liu, A. K. Engstfeld, S. Horch, B. Seger, I. E. L. Stephens, K. Chan, C. Hahn, J. K. Nørskov, T. F. Jaramillo, I. Chorkendorff, *Chem. Rev.* **2019**, *119*, 7610 – 7672.
[3] W. Luc, X. Fu, J. Shi, J. J. Lv, M. Jouny, B. H. Ko, Y. Xu, Q. Tu, X. Hu, J. Wu, Q. Yue, Y. Liu, F. Jiao, Y. Kang, *Nat. Catal.* **2019**, *2*, 423 – 430.
[4] J. J. Lv, M. Jouny, W. Luc, W. Zhu, J. J. Zhu, F. Jiao, *Adv. Mater.* **2018**, *30*, 1803111.
[5] K. P. Kuhl, E. R. Cave, D. N. Abram, T. F. Jaramillo, *Energy Environ. Sci.* **2012**, *5*, 7050 – 7059.
[6] E. L. Clark, C. Hahn, T. F. Jaramillo, A. T. Bell, *J. Am. Chem. Soc.* **2017**, *139*, 15848 – 15857.
[7] S. Ma, M. Sadakiyo, R. Luo, M. Heima, M. Yamauchi, P. J. A. Kenis, *J. Power Sources* **2016**, *301*, 219 – 228.
[8] K. J. P. Schouten, Y. Kwon, C. J. M. van der Ham, Z. Qin, M. T. M. Koper, *Chem. Sci.* **2011**, *2*, 1902 – 1909.
[9] E. L. Clark, A. T. Bell, *J. Am. Chem. Soc.* **2018**, *140*, 7012 – 7020.
[10] X. Chang, A. Malkani, X. Yang, B. Xu, *J. Am. Chem. Soc.* **2020**, *142*, 2975 – 2983.
[11] M. Jouny, W. Luc, F. Jiao, *Nat. Catal.* **2018**, *1*, 748 – 755.
[12] Y. Lum, T. Cheng, W. A. Goddard, J. W. Ager, *J. Am. Chem. Soc.* **2018**, *140*, 9337 – 9340.
[13] E. L. Clark, J. Wong, A. J. Garza, Z. Lin, M. Head-Gordon, A. T. Bell, *J. Am. Chem. Soc.* **2019**, *141*, 4191 – 4193.
[14] E. Bertheussen, A. Verdaguer-Casadevall, D. Ravasio, J. H. Montoya, D. B. Trimarco, C. Roy, S. Meier, J. Wendland, J. K. Nørskov, I. E. L. Stephens, I. Chorkendorff, *Angew. Chem. Int. Ed.* **2016**, *55*, 1450 – 1454; *Angew. Chem.* **2016**, *128*, 1472 – 1476.
[15] I. Ledezma-Yanez, E. P. Gallent, M. T. M. Koper, F. Calle-Vallejo, *Catal. Today* **2016**, *262*, 90 – 94.
[16] A. H. Wonders, T. H. M. Housmans, V. Rosca, M. T. M. Koper, *J. Appl. Electrochem.* **2006**, *36*, 1215 – 1221.
[17] P. Khanipour, M. Löffler, A. M. Reichert, F. T. Haase, K. J. J. Mayrhofer, I. Katsounaros, *Angew. Chem. Int. Ed.* **2019**, *58*, 7273 – 7277; *Angew. Chem.* **2019**, *131*, 7351 – 7355.
[18] L. Mandal, K. R. Yang, M. R. Motapothula, D. Ren, P. Lobaccaro, A. Patra, M. Sherburne, V. S. Batista, B. S. Yeo, J. W. Ager, J. Martin, T. Venkatesan, *ACS Appl. Mater. Interfaces* **2018**, *10*, 8574 – 8584.
[19] K. J. P. Schouten, Z. Qin, E. P. Gallent, M. T. M. Koper, *J. Am. Chem. Soc.* **2012**, *134*, 9864 – 9867.

Manuscript received: October 12, 2020
Accepted manuscript online: October 22, 2020
Version of record online: December 9, 2020

